Catalysis Today 156 (2010) 107–117

Contents lists available at ScienceDirect

Catalysis Today

journal homepage: www.elsevier.com/locate/cattod

Integrated analysis of a membrane-based process for hydrogen production from ethanol steam reforming

Diogo Mendes[a], Silvano Tosti[b], Fabio Borgognoni[b], Adélio Mendes[a], Luis M. Madeira[a,*]

[a] LEPAE, Chemical Engineering Department, Faculty of Engineering – University of Porto, Rua Dr. Roberto Frias, 4200-465 Porto, Portugal
[b] ENEA, Unità Tecnica Fusione, C.R. ENEA Frascati, Via E. Fermi 45, Frascati (RM) I-00044, Italy

ARTICLE INFO

Article history:
Available online 19 March 2010

Keywords:
Pd–Ag membranes
Membrane reactors
Ethanol steam reforming
Pure hydrogen
Process design

ABSTRACT

The aim of this work is to investigate the performance and energy efficiency achieved by an integrated system based on two different ethanol fuel processor configurations: a Conventional Reactor (CR) and a Membrane Reactor (MR). The CR-based configuration system consists of an ethanol reformer followed by two water-gas shift reactors operating at high and low temperatures. The final hydrogen purification is carried out by a preferential oxidizer in order to reduce the CO concentration before feeding the polymer electrolyte membrane fuel cell (PEMFC). A multi-tubular MR process using thin Pd–Ag tubes has also been considered, where the water-gas shift reaction and the hydrogen separation take place simultaneously.

The analysis showed that the MR process configuration possesses a simpler system design with a minor advantage in terms of energy efficiency (30%) compared with the conventional system (27%). Moreover, a detailed parametric analysis concerning the effects of water-to-ethanol molar ratio, reaction pressure, reformer and MR temperature, sweep-gas molar ratio and MR configuration on the achieved performance (hydrogen yield) and energy efficiency of the system has also been done.

The importance of optimizing integrated systems is shown since the optimal operating conditions from a global efficiency analysis point of view are in general distinct when compared with those obtained when focusing on the reformer reactor or individual process units alone.

1. Introduction

In recent years, the environmental sustainability has focused the attention of the researchers on the use of hydrogen as an energy vector [1]. It is being also consensual the fact that the full environmental benefit of a society transition to hydrogen is achieved only when the hydrogen needs can be derived from renewable resources, such as water photovoltaic hydrolysis or biomass gasification [2]. However, most of the hydrogen is still obtained from fossil sources [3]. Moreover, hydrogen has a very low volume density making it difficult for using in transportable devices. In this perspective, the interest of processes for producing hydrogen from reforming of ethanol, obtained by the fermentation of biomass, is growing [2,4,5]. In fact, new studies are oriented to consider the production of bio-ethanol from cellulose [6] instead of corn and sugarcane, seen as responsible for driving up the food prices as well as for giving only a slight contribution to the reduction in the greenhouse-gas emissions [7]. Additionally, bio-fuels can be used as high volume density hydrogen carriers for mobile applications. Especially for small power supplies, carbon dioxide can advantageously be released to the atmosphere, since bio-fuels are CO_2 neutral. When compared with other feedstocks (e.g., methanol, ammonia, gasoline and natural gas), bio-ethanol presents a series of advantages, since it is easier to store, handle and transport and has lower toxicity and volatility [8].

In the last years, the production of pure hydrogen from dehydrogenation reactions has been increasingly studied and applied in processes using membrane technologies. The introduction of membranes and membrane reactors in traditional processes presents several advantages such as the reduction of the number of process items, the increase of reactor performance, modularity and continuous operation [9–13]. In fact, a membrane reactor (MR) is a device where the reaction and the selective separation of one or more species take place. In the case of thermodynamic limited reactions, the selective removal of products from the reaction medium increases the conversion (shift effect) [11,13,14]. Generally, the use of a membrane selective towards hydrogen for carrying out dehydrogenation reactions (such as the reforming of hydrocarbons or alcohols) allows attaining reaction conversions higher than the thermodynamic value. In particular, the use of dense metallic membranes assures the production of ultra-pure hydrogen, avoiding the presence of any clean-up unit. This aspect is very important when the hydrogen production is aimed at feeding a polymeric electrolyte membrane fuel cell (PEMFC), which can be poisoned

* Corresponding author. Tel.: +351 22 508 1519; fax: +351 22 508 1449.
E-mail address: mmadeira@fe.up.pt (L.M. Madeira).

0920-5861/$ – see front matter © 2010 Elsevier B.V. All rights reserved.
doi:10.1016/j.cattod.2010.02.029

Nomenclature

CR	conventional reactor
E	permeability activation energy [J mol^{-1}]
E_{Nernst}	thermodynamic potential [V]
F	Faraday's constant [=96,500 C]
FC	fuel cell
$f^{in}_{H_2,a}$	hydrogen molar flow rate entering the anode [mol h^{-1}]
$f^{out}_{H_2,a}$	hydrogen molar flow rate exiting the anode [mol h^{-1}]
F_m	total mass flow rate in a given stream [g h^{-1}]
HHV	high heating value [MJ kg^{-1}]
HT-WGS	high-temperature water-gas shift
I_{cell}	current of the fuel cell stack [A]
J	hydrogen molar flux across the Pd–Ag membrane [mol m^{-2} s^{-1}]
k	rate constant (mol min^{-1} g^{-1}_{cat})
K_e	equilibrium constant
K_i	adsorption constant for species i (i = CO, H_2O, H_2 and CO_2) [atm^{-1}]
LT-WGS	low temperature water-gas shift
MR	membrane reactor
n	pressure exponent constant
$n^{reformer}_{EtOH}$	ethanol molar flow rate consumed in the reformer [mol h^{-1}]
n^{burner}_{EtOH}	ethanol molar flow rate consumed in the burner [mol h^{-1}]
P_{cell}	power of the fuel cell stack [W]
p_i	partial pressure of component i (i = CO, H_2O, H_2 and CO_2) [atm]
PEMFC	polymer electrolyte membrane fuel cell
$P_{reaction}$	reaction pressure (in the MR it refers to the lumen pressure) [MPa]
PrOx	preferential oxidation
p_1	hydrogen partial pressure at the retentate side of the Pd–Ag membrane reactor [MPa]
p_2	hydrogen partial pressure at the permeate side of the Pd–Ag membrane reactor [MPa]
R	water-to-ethanol molar ratio
$\Re$	ideal gas constant [=8.314 J mol^{-1} K^{-1}]
$-r_{CO}$	rate of reaction regarding carbon monoxide consumption (mol min^{-1} g^{-1}_{cat})
SR	steam reformer
Sweep-gas molar ratio	ratio of the sweep-gas flow rate to the ethanol flow rate incoming into the reformer unit
T	absolute temperature [K]
T_{MR}	temperature of the Membrane Reactor unit [K or °C]
T_{Ref}	temperature of the Reformer unit [K or °C]
WGS	water-gas shift
V_{cell}	fuel cell voltage [V]
$\eta_{act,an}$	anode overvoltage [V]
$\eta_{act,cat}$	cathode overvoltage [V]
η_{ohmic}	ohmic overvoltage [V]
x_i	molar fraction of component i (i = CO, H_2O, H_2 and CO_2)
Y_{H_2}	hydrogen yield (ratio of moles of hydrogen produced per mole of ethanol incoming to the reformer)
$\eta_{PEMFC\ system}$	energy efficiency of the integrated system
δ	Pd–Ag membrane thickness [m]
Φ	hydrogen permeability [mol m m^{-2} s^{-1} Pa$^{-0.5}$]
Φ_0	permeability pre-exponential factor [mol m m^{-2} s^{-1} Pa$^{-0.5}$]

by low amounts of other gases (i.e., CO concentration higher than 10 ppm [15]). Pd-based composite membranes consisting of a very thin Pd layer (in the range of few micrometers), applied by one of the several possible techniques (electroless, sputtering, CVD, etc.) over ceramic or metal porous supports, have been studied; however, the quasi-infinite hydrogen selectivity and durability seem difficult to be realized [15]. Conversely, dense metal membranes consisting of thin wall Pd–Ag permeator tubes have been produced via a cold rolling and diffusion welding procedure [16,17], where the complete hydrogen selectivity as well as the long life of the membranes has been demonstrated in long term (over 1 year) tests carried out at 250–400 °C and lumen pressures up to 2 bar [18]. The application of higher transmembrane pressures to these membranes requires the use of structured supports; a study of metal Pd-based membranes supported by stainless steel and nickel has been reported in the literature [19].

An experimental apparatus for producing pure hydrogen, that feeds a 500 W polymeric fuel cell, has been built at ENEA facilities. The experimental set-up consists of a conventional ethanol reformer followed by a Pd–Ag multi-tube membrane reactor performing both the water-gas shift reaction and the separation of the hydrogen produced [20]. However, the preliminary studies and experiments have been putting into evidence the need of considering the simulation and optimization of these innovative membrane processes, both in terms of hydrogen yield and energy efficiency integration [20].

The system integration of such membrane-based processes is rarely addressed in the literature despite its importance under the Process Intensification Strategy point of view [21]. In fact, for stationary applications the PEM fuel cells should be highly integrated systems, including a fuel processor, the fuel cell itself and a post-combustion unit that fulfils the energetic demands of the system. Therefore, the integration should not only be expressed in terms of material flows but also in terms of energy balance [22].

In this work, a membrane-based process is proposed and then compared with a heat integrated conventional process configuration. This design study starts from the analyses carried out on a hypothetical conventional process for producing hydrogen via ethanol steam reforming (SR), water-gas shift (WGS) reactors, a preferential oxidation (PrOx) unit, followed by a PEMFC stack. Following the same system design approach, a membrane-based ethanol fuel processor was implemented replacing the WGS and PrOx reactors by a unique multi-tubular Pd–Ag membrane reactor where the WGS reaction is conducted with simultaneous hydrogen purification. Commercial process simulation software (HYSYS) was used to solve the mass and energy balances, and to compute the operating conditions for each process unit [23]. The effect of key variables such as the reformer temperature, the reagents molar ratio, the reaction pressure, the temperature of the membrane reactor and the effect of sweep-gas on the fuel cell system efficiency is also discussed.

2. Description of the ethanol reformer systems

Both systems described below, CR standing for *Conventional Reactor* and MR standing for *Membrane Reactor*, have in common the following characteristics:

- a fuel processor, which chemically converts the ethanol into hydrogen, and hydrogen clean-up equipment(s);
- a fuel cell stack, which electrochemically converts the hydrogen into electric power;
- associated equipment for heat, oxygen and water management; and
- auxiliary equipment such as pumps, compressors and expanders.

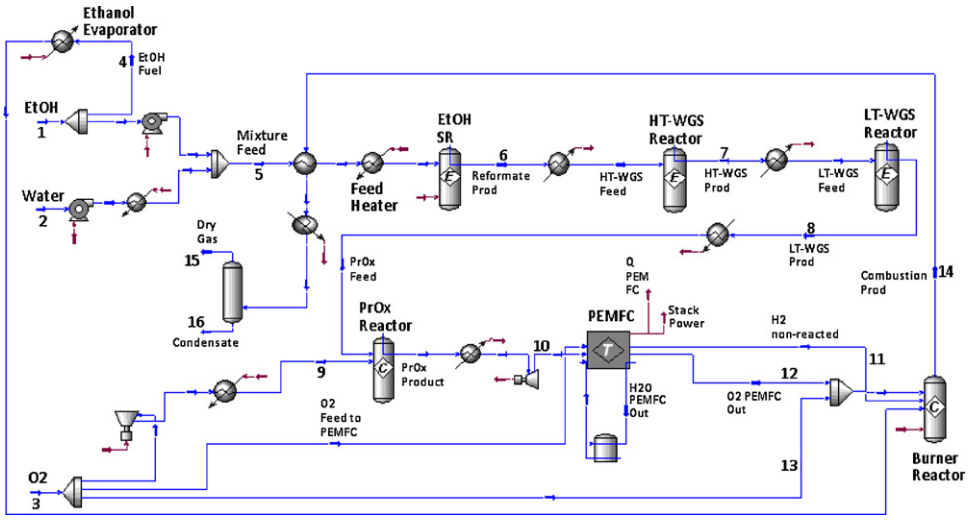

Fig. 1. Flow sheet of an integrated PEMFC system with an ethanol steam reforming system—conventional configuration.

Two different configurations were studied: (i) the conventional-based approach—CR (Fig. 1) and (ii) the membrane-based approach—MR (Fig. 2).

In terms of system design, the main difference between conventional- and membrane-based configurations is related with the hydrogen clean-up equipment(s) used and inherently on the process complexity. In the conventional configuration, three units were used to allow reaching a high H_2 content in the PEMFC feed stream: high- (HT-WGS) and low- (LT-WGS) temperature WGS reactors, and finally the PrOx unit. On other hand, in the membrane-based configuration only one unit was used—a WGS-MR.

In the simulated systems, both ethanol and water streams are provided at 20 °C and 0.1 MPa (streams 1 and 2 in Figs. 1 and 2), then are pumped to a mixer and finally fed to the ethanol reformer unit. The water flow rate required for the steam reformer is controlled by the water-to-ethanol molar ratio desired. The process design considers a burner reactor used for combusting the vent streams from the fuel processor, which is used to balance the heat demands of the system, namely for heating/vaporizing the steam reforming feed and to heat the reformer itself. The oxygen required for the combustor, fuel cell and PrOx unit in the conventional configuration system is also supplied at 0.1 MPa and 20 °C (cf. stream 3 in Fig. 1 and Table 1). A compressor is subsequently used to pressurize this stream to achieve the specified pressure and perform the CO oxidation reaction.

For simplicity, compressor, expander and pumps adiabatic efficiencies were assumed to be 75%. No pressure drops were accounted. These process systems were designed taking into account that CO_2 is separated from H_2 and dehydrated in a condenser after the burner reactor for subsequent release or capture (e.g., compression) (cf. Figs. 1 and 2).

The membrane reactor operation is simulated by an in house-designed program, as explained below, outside the simulator environment. For simplicity, this unit was represented by a "conversion reactor" (the reaction medium according to HYSYS terminology) and a splitter (the Pd–Ag membrane)—cf. Fig. 2. The operating conditions of both systems are summarised in Tables 1 and 2.

2.1. Ethanol reforming unit

The reaction pathways and thermodynamics of the ethanol steam reforming have received a significant attention in the published literature [4,8,24,25]. Moreover, the types of catalysts employed play a crucial role in the reactivity towards complete conversion of ethanol, hydrogen selectivity, and inhibition of coke

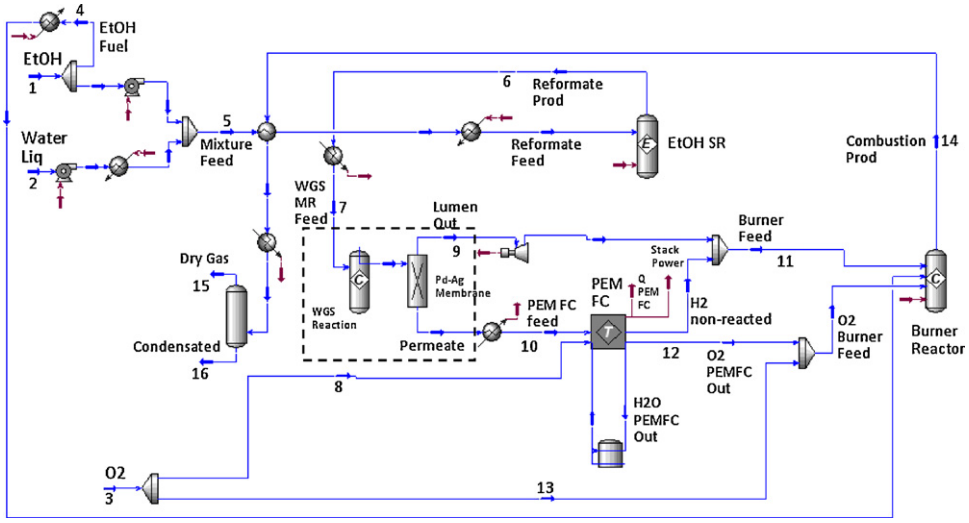

Fig. 2. Flow sheet of a PEMFC system integrated with an ethanol steam reforming system—membrane-based configuration (dotted box represents the WGS-MR).

Table 1
Operating conditions of the main streams in the CR-based system illustrated in Fig. 1 ($T_{ref.}$ = 700 °C, $P_{reaction}$ = 2 MPa and R = 3).

Stream	T [K]	P [MPa]	F_m [g h^{-1}]	x_{EtOH}	x_{H_2O}	x_{CO}	x_{H_2}	x_{CO_2}	x_{O_2}
1	293.2	0.10	141.7	1.0	–	–	–	–	–
2	293.2	0.10	134.9	–	1.0	–	–	–	–
3	293.2	0.10	604.7	–	–	–	–	–	1.0
4	293.2	0.10	26.77	1.0	–	–	–	–	–
6	973.2	2.0	250.0	3.86×10^{-3}	1.80×10^{-1}	1.69×10^{-1}	5.70×10^{-1}	7.74×10^{-2}	–
8	483.2	2.0	250.0	3.86×10^{-3}	3.56×10^{-2}	2.43×10^{-2}	7.14×10^{-1}	2.22×10^{-1}	–
10	343.2	0.10	280.6	3.86×10^{-3}	1.08×10^{-1}	9.90×10^{-7}	6.41×10^{-1}	2.46×10^{-1}	–
14	1273.2	0.10	374.7	–	4.84×10^{-1}	1.63×10^{-6}	–	5.16×10^{-1}	–
15	293.2	0.10	273.6	–	2.43×10^{-2}	–	–	9.76×10^{-1}	–
16	293.2	0.10	101.1	–	1.0	–	–	–	–

Table 2
Operating conditions of the main streams in the MR-based system illustrated in Fig. 2 (T_{ref} = 700 °C, $P_{reaction}$ = 2 MPa, T_{MR} = 360 °C and R = 3).

Stream	T [K]	P [MPa]	F_m [g h^{-1}]	x_{EtOH}	x_{H_2O}	x_{CO}	x_{H_2}	x_{CO_2}	x_{O_2}
1	293.2	0.10	132.7	1.0	–	–	–	–	–
2	293.2	0.10	134.9	–	1.0	–	–	–	–
3	293.2	0.10	555.0	–	–	–	–	–	1.0
4	293.2	0.10	17.65	1.0	–	–	–	–	–
6	973.2	2.0	250.0	3.86×10^{-3}	1.80×10^{-1}	1.69×10^{-1}	5.70×10^{-1}	7.74×10^{-2}	–
9	633.2	2.0	221.7	1.36×10^{-2}	6.67×10^{-2}	2.66×10^{-2}	4.99×10^{-2}	8.43×10^{-1}	–
10	633.2	0.10	28.44	–	–	–	1.0	–	–
14	1273.2	0.10	364.2		5.18×10^{-1}	1.24×10^{-2}		4.70×10^{-1}	–
15	293.2	0.10	253.4		1.28×10^{-2}	2.53×10^{-2}		9.62×10^{-1}	–
16	293.2	0.10	110.7	–	1.0	–	–	–	–

formation. Non-noble metal, such as Ni-based catalysts, are promising materials to conduct the reaction due to their relative low-cost, high activity, selectivity to H_2 and stability [4]. In the present study, the steam reforming of ethanol is considered as an ideal case, where no intermediate compounds are formed, as previously suggested by Song et al. [26]. Furthermore, each reaction step described by reactions (1) and (2) is considered to be at equilibrium conditions at the reactor outlet.

Ethanol decomposition reaction:

$$C_2H_5OH + 3H_2O \leftrightarrow 2CO_2 + 6H_2, \quad \Delta H^0_{298\ K} = 170.41\ \text{kJ mol}^{-1} \quad (1)$$

Reverse water-gas shift (WGS) reaction:

$$CO_2 + H_2 \leftrightarrow CO + H_2O, \quad \Delta H^0_{298\ K} = 41.1\ \text{kJ mol}^{-1} \quad (2)$$

The dependence of the equilibrium constants with temperature for reactions (1) and (2) have been provided by Semelsberger et al. [27] and Moe [28], respectively. The equilibrium constants for each reaction (K_e) were then interpolated by HYSYS, obtaining for each reaction a linear equation of the type:

$$\ln(K_e) = A + B\ T^{-1} + C\ \ln(T) + D\,T \quad (3)$$

The values of the parameters are described in Table 3.

The reactor is assumed to be isothermal, meaning that heat has to be supplied from an external energy source to maintain the temperature. In conventional tubular steam reforming adopted for both the CR and the MR configuration, the energy required to drive the endothermic reforming reactions is assumed to be supplied by the combustion of a portion of fuel outside the reactor, *cf.* Figs. 1 and 2.

2.2. Water-gas shift reaction unit

Typically, gas can emerge from the reformer with a CO level of 1–10 vol.%, which gets adsorbed on the noble catalyst of the PEMFC, poisoning it. Therefore, the fuel processor must be designed to convert the CO content in the fuel stream to levels that are tolerated by the Pt catalyst of the PEMFC; moreover, the high conversion of CO increases the hydrogen yield. This task is partially accomplished by the water-gas shift reactors, where the following reaction takes place:

$$CO + H_2O \leftrightarrow CO_2 + H_2, \quad \Delta H^0_{298\ K} = -41.1\ \text{kJ mol}^{-1} \quad (4)$$

The performance of these units depends on the input concentration of CO and H_2O/CO ratio. Such variables are in turn related to the reformer reaction pathway as well as to the water-to-ethanol molar ratio (R), reformer unit temperature (T_{Ref}), and reaction pressure ($P_{reaction}$), which parametric analysis is done below. Besides, the temperature of the WGS reaction unit affects its performance because it modifies the CO conversion.

2.2.1. Conventional configuration

In the conventional configuration (Fig. 1), the WGS reaction was assumed to be carried out, as usual, in two adiabatic shift reactors in series with an inter-cooler in between. This allows a smaller adiabatic temperature rise and a better steam management, therefore making the process more economical [29]. These units perform the exothermal WGS reaction that is considered to be at equilibrium conditions at the reactor outlet. The HYSYS library was used to obtain the equilibrium data for the reaction. The first WGS stage is characterized by working at higher temperatures, favoring a fast CO consumption and minimizing the catalyst bed volume, and it is called the high-temperature shift (HT-WGS) reactor. A chromium-promoted iron oxide catalyst is assumed to be used in the HT-WGS reactor. In the next stage the reaction takes place at a lower temperature for obtaining a higher CO conversion, which is limited by the thermodynamic equilibrium of the exothermal WGS reaction. An inter-stage cooling system was thus used to operate the second WGS reactor at a lower temperature. A copper–zinc–alumina cata-

Table 3
Values of the estimated parameters in Eq. (3) for reactions (1) and (2).

Reaction	A	B [K]	C	D [K^{-1}]
$C_2H_5OH + 3H_2O \leftrightarrow 2CO_2 + 6H_2$	4.740×10^{1}	-2.276×10^{4}	–	2.359×10^{-3}
$CO_2 + H_2 \leftrightarrow CO + H_2O$	5.268×10^{-1}	-4.380×10^{3}	5.809×10^{-1}	-4.066×10^{-4}

lyst is usually employed in the LT stage. In this study it was assumed that the HT- and the LT-WGS reactors operate at 360 °C and 210 °C, respectively [30].

2.2.2. Membrane-based configuration

In the membrane-based configuration (Fig. 2) the WGS reaction was supposed to be carried out in an adiabatic multi-tube membrane reactor. A membrane reactor consisting of 19 Pd–Ag thin wall tubes has been considered for the simulation work. These permeator tubes of 10 mm of internal diameter, wall thickness of 0.050 mm and 250 mm of length can be produced by cold rolling and diffusion welding of metal foils made of a Pd alloy with Ag 20–25 wt.%. Such a multi-tube membrane module has been built at ENEA laboratories and should be coupled with a 500 W PEM fuel cell. The catalyst bed is assumed to be inserted in the membrane lumen and the permeated hydrogen is collected in the shell side at 0.1 MPa. The permeate stream formed by pure H_2 is then fed to the PEMFC stack. The retentate stream, i.e., essentially the produced CO_2, the CO not eliminated and the H_2 not permeated (stream number 9 in Fig. 2), is conducted to the combustion unit to fulfil the energetic needs of the system. The energy released by the expander unit, when the WGS-MR is operated at pressures higher than 0.1 MPa, was not taken into consideration in the energy balance.

A computer code developed for simulating a WGS-MR of one membrane tube has been used [31]. The model accounts for the kinetics of the WGS reaction over an iron-based catalyst and the hydrogen transport (permeation) through the Pd–Ag membrane. A Langmuir–Hinshelwood kinetic model was used based on the surface reaction of molecularly adsorbed reactants as the rate determining step, which leads to the following expression of the reaction rate:

$$-r_{CO} = \frac{kK_{CO_2}K_{H_2O}(p_{CO}p_{H_2O} - (p_{CO_2}p_{H_2}/K_e))}{(1 + K_{CO}p_{CO} + K_{H_2O}p_{H_2O} + K_{CO_2}p_{CO_2})^2} \quad (5)$$

where $-r_{CO}$ is the rate of carbon monoxide consumption (mol min^{-1} g_{cat}^{-1}), k is the rate constant, K_e is the equilibrium constant, K_i is the adsorption constant for species i (i = CO, H_2O, H_2 and CO_2) and p_i is the partial pressure of the component i. The kinetic constants have been evaluated by Podolski and Kim [32] with a 93% iron and 7% chromium catalyst:

$$k = \exp\left(-\frac{2456}{T} + 20.292\right) \text{ mol min}^{-1} \text{ g}_{cat}^{-1} \quad (6)$$

$$K_{CO} = \exp\left(\frac{1542}{T} - 3.392\right) \text{ atm}^{-1} \quad (7)$$

$$K_{H_2O} = \exp\left(\frac{3128}{T} + 6.426\right) \text{ atm}^{-1} \quad (8)$$

$$K_{CO_2} = \exp\left(\frac{6312}{T} - 9.285\right) \text{ atm}^{-1} \quad (9)$$

The MR model is based on the following main assumptions: steady-state conditions, plug-flow, isothermal operation, ideal gas behavior, negligible pressure drops, negligible radial temperature and concentration profiles (one dimensional model—negligible concentration polarization).

Pressure drop is not of concern as it is typically negligible in the range of flow rates that are usual for the application of the reactor [20]. Besides, all other hypotheses are in principle valid for the dimensions of the set-up considered (i.e., for coupling to a 500 W PEM fuel cell).

The tubular membrane reactor is divided into finite volume elements where the composition of the gas, reaction rate and permeability towards hydrogen can be considered constant. Assuming as inlet boundary conditions for each volume the outlet values of the previous one, the mass balance for each component of the mixture is performed. The computation of mass balances, both at the retentate and at the permeate side of the reactor, requires the evaluation of reaction rate and permeation rate. These, in turn, depend on the partial pressures of the gases in the reactor. Moreover, the permeation rate depends on the partial pressure of hydrogen at the permeate side of the reactor. Therefore, an iterative method of computation has been set up, as described elsewhere [31]. The calculation is iterated up to convergence (error $<1 \times 10^{-10}$ mol s^{-1}).

Using the code, the molar flow rates of the gaseous species inside each permeator tube of the membrane reactor have been evaluated.

2.3. Preferential oxidation reactor

In the CR configuration, due to the WGS reaction equilibrium limitations, the LT-WGS reactor typically achieves a residual CO concentration in the order of 0.5–1.5 dry vol.%. Thus, the preferential oxidation (PrOx) unit is used to bring down to ppm levels the CO concentration (cf. Fig. 1). Supported noble metal catalysts are typically used to promote the reaction, in particular, platinum/alumina [33]. The precious metals used are efficient, but only start to be active at about 170 °C. Additionally, they are not active at low O_2/CO ratios because O_2 and CO compete for the same sites. Therefore, air is added in slight excess, and so is normal that a small amount of hydrogen is oxidized. In this reactor, the oxidation of CO using oxygen proceeds according with the following reaction:

$$CO + \tfrac{1}{2}O_2 \rightarrow CO_2, \quad \Delta H^0_{298\ K} = -283.2 \text{ kJ mol}^{-1} \quad (10)$$

As mentioned previously, the selectivity of the catalyst will typically not avoid the combustion of some hydrogen that is present in the gas stream through the following reaction:

$$H_2 + \tfrac{1}{2}O_2 \rightarrow H_2O, \quad \Delta H^0_{298\ K} = -241.0 \text{ kJ mol}^{-1} \quad (11)$$

In this study, the O_2 inlet flow is computed as a function of the CO flow rate assuming the requirement of two moles of O_2 per mole of CO [34]. In the model, the CO oxidation is considered completed after reaching 10 ppm at the reactor's outlet. Since this combination of specifications cannot be solved directly, the Adjust operation of HYSYS was used to automatically conduct the trial-and-error iterations. The remaining O_2 reacts totally with hydrogen, which represents a selectivity (mol H_2 consumed per mol CO consumed) of nearly 3 [34]. An adiabatic operation at a temperature of 200 °C has been considered for the PrOx reactor [35,36].

2.4. Polymer electrolyte membrane fuel cell stack

To investigate the performance of a PEMFC system, an equilibrium-based electrochemical model has been employed [22,34]. The basic expression for the voltage for a single cell is:

$$V_{cell} = E_{Nernst} + \eta_{act,an} + \eta_{act,cat} + \eta_{ohmic} \quad (12)$$

where E_{Nernst} is the thermodynamic potential, $\eta_{act,an}$ is the anode overvoltage, a measure of the voltage loss associated with the anode, $\eta_{act,cat}$ is the cathode overvoltage, a measure of the voltage loss associated with the cathode, and η_{ohmic} is the ohmic overvoltage, i.e., the internal losses associated with the proton conductivity of the electrolyte and electronic internal resistances. The three overvoltage terms are all negative in the above expression and represent reductions from E_{Nernst} to give the real cell voltage, V_{cell}. For simplification, the operating voltage was set at 0.5 V [26,34,37].

The current, I_{cell}, is related with the hydrogen molar flow rate that is consumed at the anode:

$$I_{cell} = 2F\left(f^{in}_{H_2,a} - f^{out}_{H_2,a}\right) \quad (13)$$

where F is the Faraday constant (96,500 C).

The actual electrical power generated by the cell (P_{cell}) can then be calculated from:

$$P_{cell} = V_{cell}\ I_{cell} \quad (14)$$

It is assumed that the cell operates with the inlet oxidant fed to the cathode humidified at a relative humidity of 80%. The PEM is considered to be isothermal and isobaric. A pressure of 0.1 MPa and a fuel cell temperature of 70 °C are assumed. The fuel utilization is considered to be 80% [34] and the oxygen fed to the PEMFC is supplied with 30% of excess concerning the inlet H_2.

2.5. Post-combustion unit

The addition of a burner reactor for converting the vented fuel from the PEMFC (cf. Figs. 1 and 2) can improve the energy efficiency of the system by providing most of the heat needs [38]. Therefore, in this study, the generated heat obtained in the post-combustion unit (operating at 1000 °C and 0.1 MPa) is used to balance the energy requirement of the overall fuel processing system. Supplementary firing of ethanol is considered if the energy content of the vented fuel is not sufficient to close the energetic balance. Some assumptions were made:

- The combustion is complete and
- Stoichiometric combustion has been considered accordingly with the following reaction:

$$C_2H_5OH + 3O_2 \rightarrow 2CO_2 + 3H_2O, \quad \Delta H^0_{298\ K} = -1275.56\ \text{kJ mol}^{-1} \quad (15)$$

Finally, concerning the heat exchange, the steam reforming unit is the only reactor which consumes energy due to the endothermic characteristic of the reaction set. There is also energy consumption for heating the feed and the evaporation of the additional ethanol that is fired, prior to entering the reactors, and for auxiliary equipment such as pumps and compressors (cf. Figs. 1 and 2).

2.6. Definition of the fuel cell system efficiency

Concerning the evaluation of the overall efficiency of the integrated systems, an expression was formulated where the energy output obtained by the PEMFC is divided by the heating value of the ethanol consumed in the fuel processor for reforming ($n^{reformer}_{EtOH}$) and burning unit (n^{burner}_{EtOH}):

$$\eta_{PEMFC\ system} = \frac{P_{cell}}{\left(n^{reformer}_{EtOH} + n^{burner}_{EtOH}\right) HV_{EtOH}} \quad (16)$$

The higher heating value (HHV) was used as the HV factor, representing the amount of heat produced by the complete combustion of the fuel (initial and final states at standard conditions). The value of 1300 kJ mol^{-1} was then considered.

3. Results and discussion

The two integrated process models have been used to determine the effect of the most relevant operating conditions. The influence of the water-to-ethanol molar ratio, reforming and membrane reactor temperature, reaction pressure and sweep-gas were studied in terms of ethanol fuel processor performance as well as in terms of overall energy efficiency.

3.1. Influence of the water-to-ethanol molar ratio and reaction pressure

In this section, the effects of the water-to-ethanol molar ratio (R) and reaction pressure are investigated. Fig. 3 presents the reactors' yields and the total yield of the integrated ethanol fuel processor for the conventional and membrane-based configuration systems. These yields are computed as the ratio of moles of hydrogen produced per mole of ethanol incoming to the reformer (Y_{H_2}).

In this study, the performance in terms of the total H_2 yield for both ethanol fuel processor configurations is favored for higher water-to-ethanol molar ratios (Fig. 3). Due to the water excess, the thermodynamic equilibrium conversion of the ethanol reforming reaction enhances the H_2 production and penalizes the CO concentration at the outlet stream of the unit (cf. Eqs. (1) and (2)); therefore, in both processors, the WGS step produces less hydrogen. Moreover, in the WGS membrane reactor the hydrogen yield significantly decreases with the feed molar ratio. In fact, an excess of water reduces the hydrogen partial pressure and inherently the H_2 recovery, decreasing the CO shift effect. In a conventional ethanol fuel processor, due to the lower CO formation at the reformer section, the performance of the PrOx reactor improves, consuming less H_2.

The total H_2 yields attained in both fuel processor configurations are very similar at high water-to-ethanol molar ratios (Fig. 3). However, a slight difference is noted in the conventional processor, particularly at the lowest water-to-ethanol molar ratios, where a higher amount of H_2 is consumed during the oxidation of CO at the PrOx unit.

In both configurations, the largest contribution to the H_2 yield is, as expected, due to the reformer. Nevertheless, the WGS reactor(s) contribution cannot be neglected, accounting up to 28% (for R = 3 and $P_{reaction}$ = 0.1 MPa) in the conventional unit and up to 22% (for R = 3 and $P_{reaction}$ = 2 MPa) in the MR-based one. The reaction

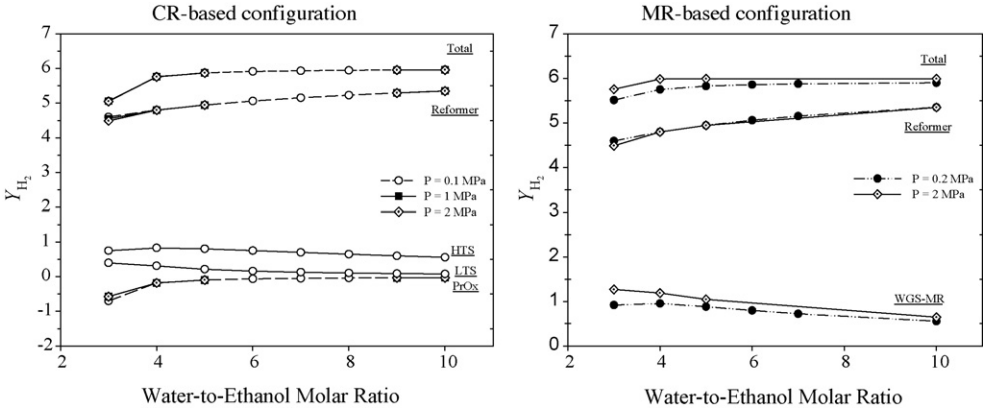

Fig. 3. Reactors yields vs. water-to-ethanol molar ratio at different reaction pressures (T_{Ref} = 700 °C and T_{MR} = 360 °C).

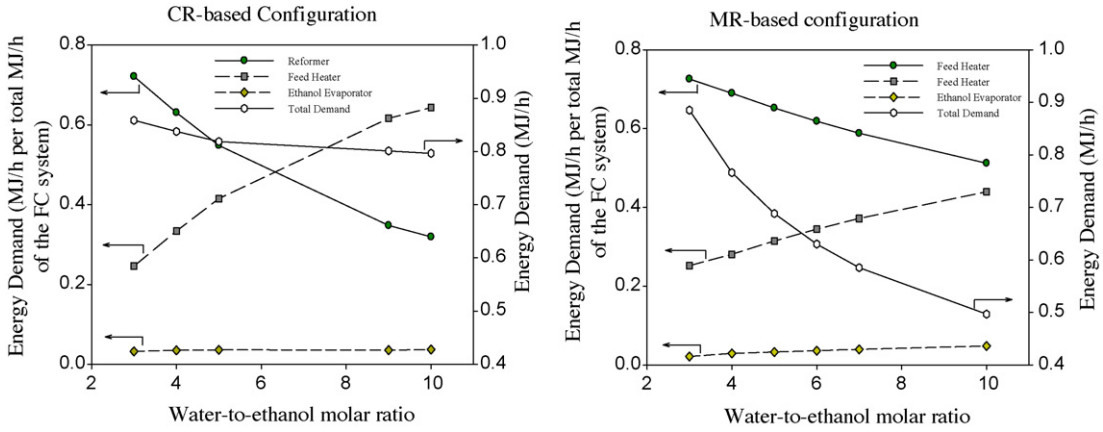

Fig. 4. The effect of the water-to-ethanol molar ratio (R) on the energy demand of the system ($P_{reaction}$ = 2 MPa, T_{Ref} = 700 °C and T_{MR} = 360 °C).

pressure has distinct effects in both fuel processors, as shown also in Fig. 3. In the case of the conventional one, the total H_2 yield is almost insensitive to the pressure variation in the range studied (0.1–2 MPa). This is related with the fact that the ethanol decomposition achieves 100% conversion for $R > 4$, whatever is the reaction pressure. For $R < 4$ there is an increasing slight negative influence of the pressure, as predicted from the Le Chatelier's principle (because there is an increase in the total number of moles—cf. Eq (1)). On the other hand, the overall performance of the membrane-based fuel processor increases with the reaction pressure. Since the pressure gradient across the membrane increases, the H_2 permeation through the membrane is favored, shifting the WGS reaction equilibrium towards additional formation of H_2.

Fig. 4 presents the energy demand of the reforming reactor, feed heater and ethanol evaporator of each integrated system versus the water-to-ethanol molar ratio at a constant reforming temperature and reaction pressure (T_{ref} = 700 °C and $P_{reaction}$ = 2 MPa). The energy demand evaluation of a MR-based system should be performed at conditions of high hydrogen recovery.

Despite the high H_2 yields obtained for both fuel processors for $R > 4$—Fig. 3, the higher water feed flow rate demands extra energy for feed heating and vaporizing, Fig. 4. Therefore, additional ethanol should be furnished to the system, decreasing the energy efficiency, as described later on. The maximum energy demand is, however, located at the minimum water-to-ethanol molar ratio due to the high energy consumptions in the reformer unit. In opposition, at these conditions the energy efficiency is maximized since the amount of H_2 supplied to the PEMFC becomes higher.

Comparing both system configurations, it is worth mentioning that when increasing the reactants molar ratio the MR-based configuration system shows a lower overall energy demand (cf. Fig. 4). This fact is justified by the lower H_2 recovery in the MR that follows the increase on the water-to-ethanol molar ratio; by increasing the water-to-ethanol molar ratio the enthalpy content of the stream exiting the burner is therefore higher, favoring this way the heat exchanger performance.

In Fig. 5, a 3D surface is presented where the global efficiency of the system based on the HHV is shown. The energy efficiency is presented as a function of the water-to-ethanol molar ratio and reaction pressure. Comparing both configurations, it can be seen that only a minor increase on the energy efficiencies can be obtained in the membrane-based configuration system. Particularly, at a reformer temperature of 700 °C, a maximum efficiency of 29.1% is achieved at R = 3 and $P_{reaction}$ = 2 MPa and of 27.3% at R = 4 and $P_{reaction}$ = 0.1 MPa for the MR- and CR-based configurations, respectively (cf. Fig. 5).

In the work by Benito et al. [38], a conventional bio-ethanol processor-PEMFC system, with heat integration, was proposed and evaluated. A similar theoretical energy efficiency to the one reported by us was obtained by these authors. Higher energy

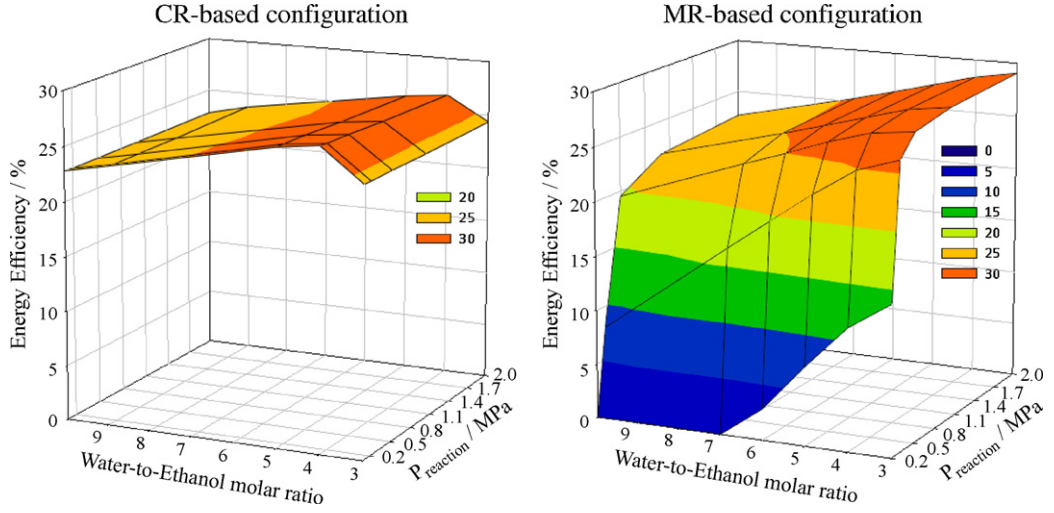

Fig. 5. Effect of the water-to-ethanol molar ratio and reaction pressure on the overall energy efficiency (T_{Ref} = 700 °C and T_{MR} = 360 °C).

efficiency values for CR configurations can be, however, found in the literature. For example, Francesconi et al. [34], Godat and Marechal [22] and Perna [39] obtained maximum energy efficiencies of around 36%, 46% and 43%, respectively. The difference of such values compared with the ones obtained in this work, for the CR system, is related with the different operating conditions and fuel cell system modeled (e.g., fuel utilization factor, fuel cell temperature and pressure and real cell voltage). Moreover, also different heat exchange networks were considered, which leads to different efficiencies of the FC systems configuration.

From Fig. 5 it is also possible to conclude that the membrane-based configuration is more affected by the operating conditions used than the conventional one. In fact, $R = 3$ favors the MR-based system where a higher H_2 partial pressure is obtained at the outlet stream of the reformer. Therefore, a higher H_2 recovery is obtained at the permeate stream of the MR, which leads to an increase of the power output. However, when changing the other parameter, i.e., the reaction pressure, one can see that it might have a tremendous effect on the energy efficiency of the MR-based unit (cf. Fig. 5). In the MR-based system, since the H_2 permeation flux depends on the H_2 partial pressure gradient across the membrane, it is expected that the increase of the reaction pressure favors the fuel cell output power and synergistically the energy efficiency of the system. In limiting cases, i.e., when the reaction pressure tends to be very low but the water-to-ethanol molar ratio is simultaneously high ($R \geq 7$), null efficiencies are obtained. On the other hand, the effect of the reaction pressure on the CR-based system is almost negligible, while the influence of R is a bit more notorious. The optimum in the energy efficiency for $R \approx 4$ results from the combination of two facts: by decreasing R, higher amounts of hydrogen are obtained (because the equilibrium conversion effect is almost negligible), however for low R values a more significant consumption of hydrogen occurs in the PrOx unit.

At lower water-to-ethanol molar ratio values, especially for $R < 3$, there is the formation of coke over the steam reforming catalyst. Coke can "destroy" the catalyst structure and occupy the catalyst surface, reducing the catalyst activity; besides, the H_2 yield of the process becomes severely reduced due to the formation of by-products. So, higher water-to-ethanol molar ratios are frequently employed in practice to reduce the rate of carbon deposition and favor the H_2 production. Even at a H_2O/C_2H_5OH molar ratio of 5, the MR-based system shows an energy efficiency that is very close to the CR configuration, when operated at a relatively high reaction pressure—Fig. 5. The reaction pressure is certainly an important design variable of the MR-based system, although above 0.5 MPa the energy efficiency increases only marginally.

It is worth noting that the optimal water-to-ethanol molar ratio and reaction pressure, considering the reformer alone and the total H_2 yields achieved for each fuel processor configuration (Fig. 3), does not agree with the best operating conditions from the point of view of a global efficiency analysis (cf. Figs. 4 and 5). This fact indicates the importance of optimizing integrated systems rather than optimizing process units separately for different objective functions, as also indicated by Francesconi et al. [34].

Up to now, the MR-based system configuration revealed to be promising in terms of both performance and efficiency for the range of conditions studied when compared with the conventional process. Despite the advantages of using the MR-based process, a decisive selection between both systems should be made on the basis of an economic balance considering the investment, capital and operation costs involved in each one. The membrane reactor is probably the most expensive piece of equipment because it uses 50-μm thick palladium-based membranes. However, much thinner membranes are being developed and it is expected that a composite palladium membrane 1 μm tick costs only 50–100% more than the corresponding ceramic support.

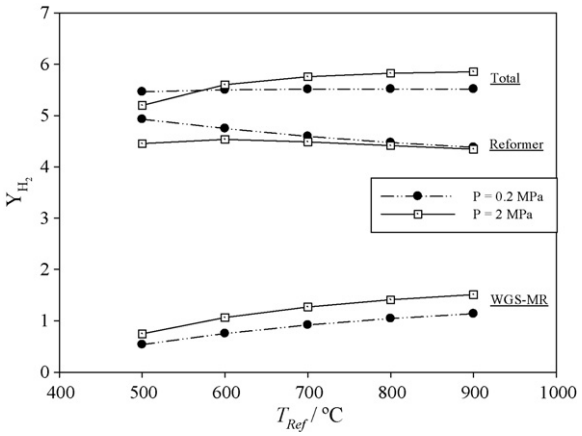

Fig. 6. Reactors yields vs. temperature of the reformer at different reaction pressures for the MR-based process ($R = 3$ and $T_{MR} = 360\,^{\circ}C$).

In the following sections, the MR-based system will be studied in more detail in order to investigate the effects of some other operating conditions.

3.2. Influence of the reformer temperature

To reduce the operating costs and increase the energy efficiency of the FC system, a compromise should be made between the temperature and pressure at the reformer unit; this should take into account the H_2 yields obtained by the fuel processor and the temperature limit at which coke formation is negligible.

The effect of the reforming temperature on the MR-based configuration is analyzed in this section considering $R = 3$. The H_2 yield of the fuel processor plot (Fig. 6) shows that increasing the temperature, the total hydrogen production increases, which is in opposition to the performance behavior of the reformer unit. The ethanol steam reforming is an equilibrium-limited reaction. Due to its endothermicity, temperature has a positive effect on the ethanol conversion. In the range of temperatures considered, the H_2 yield in the reformer unit is, however, negatively affected. This happens because the equilibrium conversion of reaction (1) (which is close to completion) is less affected by this variable than the equilibrium conversion of reaction (2). In particular, the equilibrium conversion for the ethanol decomposition increases from 98.39% ($R = 3$, $P_{reaction} = 0.2$ MPa and $T_{ref} = 500\,^{\circ}C$) to 99.85% ($R = 3$, $P_{reaction} = 0.2$ MPa and $T_{ref} = 900\,^{\circ}C$). For the RWGS reaction, the conversion increases from 49.58% to 80.56%, in the same temperature range (and equal conditions). This way, the effect on the RWGS overcomes the 6 mol of H_2 produced for each mol of ethanol consumed through reaction (1). Since the CO content is increased by the effect of T_{ref}, the H_2 production of the fuel processor is then mainly favored via the WGS reaction (cf. Fig. 6). Globally, the H_2 production of the fuel processor is favored by the reformer temperature. This fact is more evident at higher reaction pressures, where the H_2 recovery and CO shift is higher. At lower pressures (e.g., 0.2 MPa in Fig. 6), the positive effect reached in the WGS-MR is offset by the negative effect in the reformer, being the overall H_2 yield nearly independent of the reformer temperature.

In Fig. 7, the energy efficiency of the MR system is shown as a function of the water-to-ethanol ratio and reforming temperature at 2.0 MPa (high H_2 recovery conditions). Higher energy efficiencies are obtained at lower reformer temperatures because of the smaller energy requirements in the reactor and evaporation. A maximum efficiency of $\eta_{PEMFC\ system} = 30.2\%$ occurs at the minimum temperature (500 °C) of the reformer considered in this study. Additionally, at these conditions, no supplementary firing of ethanol is necessary.

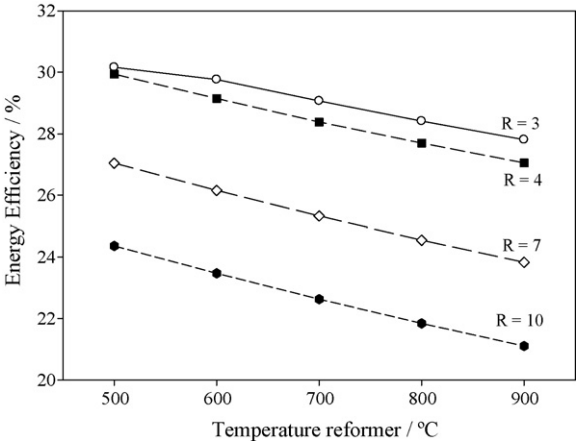

Fig. 7. The effect of the water-to-ethanol molar ratio and reformer temperature on the energy efficiency of the fuel cell system for the MR-based system ($P_{reaction}$ = 2 MPa and T_{MR} = 360 °C).

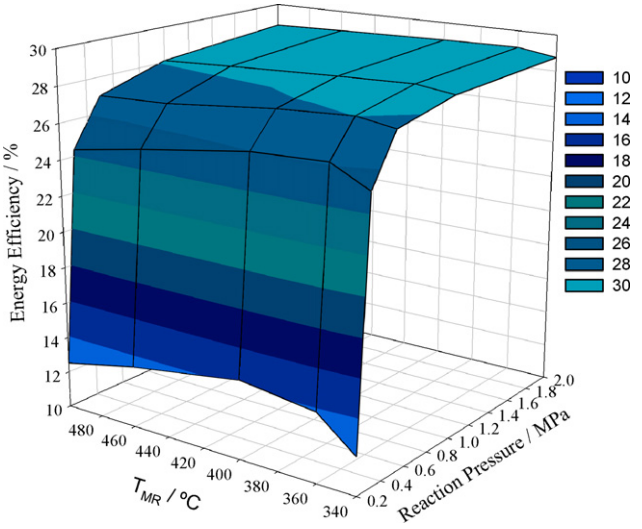

Fig. 9. The effect of the reaction pressure and temperature of the MR on the energy efficiency of the fuel cell system (T_{Ref} = 700 °C, R = 3).

Ethanol steam reforming operation at 500 °C or below is experimentally described in the literature as a promising choice for fuel cell applications. The effect of R in the energetic efficiency is similar to that reported in Fig. 5 (i.e., the smaller the water-to-methanol ratio, the higher the efficiency because more H_2 is produced).

3.3. Influence of the WGS-MR temperature

In this section, the reactor's performance and the global energy efficiency of the system are studied as a function of the WGS-MR temperature.

The hydrogen diffusion through palladium occurs via a solution/diffusion mechanism, which is frequently described as follows [40]:

$$J = \frac{\Phi}{\delta}\ (p_1^n - p_2^n) \tag{17}$$

where J is the hydrogen permeation flux (mol m^{-2} s^{-1}), Φ is the hydrogen permeability (mol m m^{-2} s^{-1} Pa^{-n}), δ is the metal wall thickness (m), n is a model constant (n = 0.5 assuming Sieverts' law), and p_1 and p_2 (Pa) are the hydrogen partial pressures upstream and downstream, respectively (i.e., in the lumen and permeate sides, respectively). Moreover, the hydrogen transport through the dense palladium-based membrane is an activated process. Assuming that the permeability follows the Arrhenius' law, it can be written:

$$\Phi = \Phi_0\ e^{-(E/\Re T)} \tag{18}$$

where Φ_0 is the pre-exponential factor (mol m m^{-2} s^{-1} Pa$^{-0.5}$), E is the activation energy (J mol^{-1}), $\Re$ is the gas constant and T (K) is the absolute temperature. The hydrogen permeability parameters of the Pd–Ag 23 wt.% alloy have been obtained from the literature [31]: $\Phi_0 = 7.730 \times 10^{-8}$ mol m m^{-2} s^{-1} Pa$^{-0.5}$ and $E = 6.601 \times 10^3$ J mol^{-1}.

The hydrogen permeation is then expected to increase with the temperature and transmembrane hydrogen partial pressure difference. Therefore, it is important to evaluate the influence of these variables on the global performance of the MR-based system.

In Figs. 8 and 9, the effect of the WGS-MR temperature and reaction pressure on the global H_2 yield, CO conversion, H_2 recovery and energy efficiency are shown; a water-to-ethanol molar ratio of 3 and a reformer temperature of 700 °C were considered.

Fig. 8a shows that increasing the temperature of the WGS-MR, the hydrogen total yield of the fuel processor has a maximum value at 360 °C, within the pressure range presented in this study (although more easily noticed in the figure at $P_{reaction}$ = 2 bar). This result is explained by the combined effect that the CO conversion and the H_2 recovery attained in the WGS-MR have with the temperature (see Fig. 8b). In other words, due to the exothermicity of the WGS reaction, temperature negatively affects the thermodynamic CO conversion level based in the feed conditions. However, the shift effect is enhanced by the increase of the H_2 recovery, which is favored by the temperature (see Eq. (18)). Therefore, an optimal temperature of the WGS-MR can be obtained in order to achieve the maximum CO conversion and inherently the global H_2 yield.

The relationship between the catalyst activity and the membrane permeation is quite important on the optimization of the

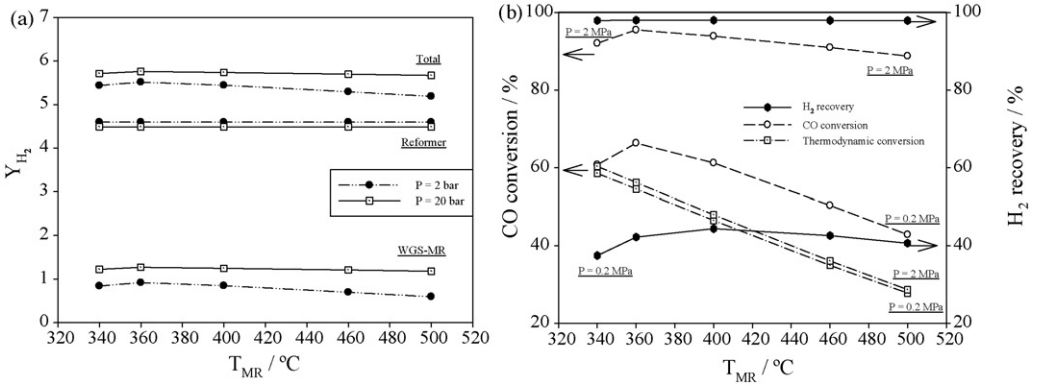

Fig. 8. The influence of the WGS-MR temperature on (a) the H_2 yield and (b) CO conversion and H_2 recovery at different pressures (T_{Ref} = 700 °C, R = 3).

membrane reactor. Despite the work performed being related to a functional model under development at ENEA, the optimization of the reactor area/volume aspect ratio can be done using the Damköler–Permeation (DaPe) number [41]. The membrane is needed to permeate hydrogen produced from CO conversion, which reaction takes place in the fixed bed delimited by the membrane walls. Fig. 8b plots CO conversion and recovered hydrogen as a function of the MR temperature. From this figure it can be seen that most of the produced hydrogen is recovered, indicating that the reactor aspect ratio is adequate.

From Fig. 8b, it can be seen that the total CO conversion was not achieved for the WGS-MR module and operating conditions simulated. In other words, a retentate stream containing mainly CO_2, some steam, non-recovered hydrogen and the non-converted CO (Table 2) is obtained. This indicates that improvements should be made in the module membrane (e.g., higher permeation area and/or lower membrane thickness) and/or in the process conditions (e.g., using a higher reaction pressure) to improve the H_2 recovery and the remaining CO consumption.

The WGS-MR shows higher energy efficiencies for 360 °C, where the H_2 production is favored, and for reaction pressures above 0.5 MPa (Fig. 9). A compromise should then exist between the WGS-MR temperature and the lumen (retentate) side pressure, in order to achieve higher performances and global energy efficiencies.

3.4. Influence of the sweep-gas and MR configuration

Up to this point, we assumed that the WGS-MR operates without sweep-gas in the permeate side, which was settled as ambient pressure. Despite the higher simplicity of the process in terms of final H_2 purification and cost, these are very limiting conditions for the H_2 recovery and yield. This limitation can be overcome by applying vacuum to the permeate side or by feeding a sweep-gas to the permeate chamber (shell side) of the membrane module.

In a previous work by Tosti et al. [20], the authors concluded that the permeating hydrogen should be collected in the shell side using a sweep-gas stream in counter-current mode for increasing the permeation driving force.

Using steam as sweep-gas has the advantage of being usually available on-site and being easily separated from the permeated hydrogen; alternatively, the hydrogen humidified stream could be directly fed to the fuel cell [42]. Often, the higher the sweep-gas flow rate, the greater the permeation rate. However, the vaporization of water is one of the most energy intensive operations in industry. Therefore, the flow rate of water sweep-gas should be studied not only in terms of the H_2 recovery achieved in the MR, but also in terms of the energy efficiency of the system.

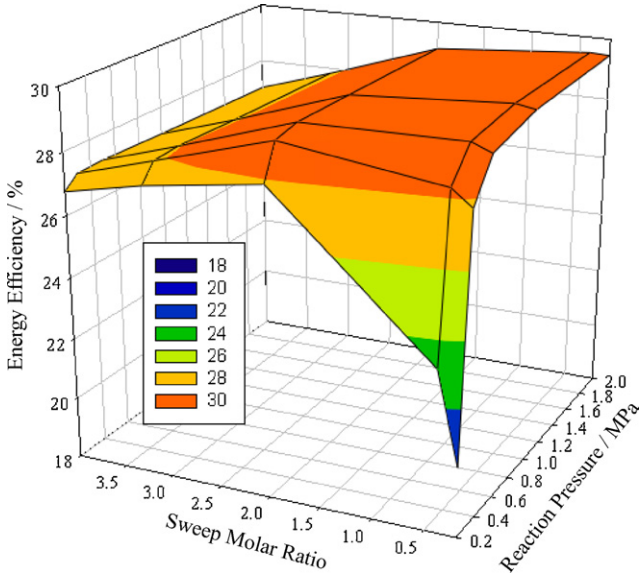

Fig. 10. The effect of the steam sweep-gas molar ratio and reaction pressure on the global energy efficiency. Operating conditions are: the steam sweep-gas is fed in counter-current mode and T_{ref} = 700 °C, R = 3 and T_{MR} = 360 °C.

Taking this into consideration, Fig. 10 shows the effect of the sweep-gas molar ratio (ratio of the steam sweep flow rate to the ethanol flow rate incoming into the reformer unit) over the energy efficiency of system, at different retentate pressures. The role of the steam sweep-gas molar ratio on the energy efficiency of the system clearly depends on the pressure of the WGS-MR retentate/reaction side. At low reaction pressures, where the pressure gradient across the membrane is low and inherently the H_2 recovery, higher energy efficiencies are in principle favored by the usage of a higher steam sweep molar ratio. However, once attained the maximum energy efficiency, the increase of the sweep molar ratio, despite the enhancement of the H_2 recovery, is no longer advantageous (cf. Fig. 10). Extra energy is then necessary to vaporize the sweep-gas water, decreasing the energy efficiency of the system. When operating at higher reaction pressures, a lower amount of sweep-gas is needed to achieve higher energy efficiency.

At this point it is interesting to analyze the improvements obtained using the steam sweep-gas compared with no sweep-gas. In Fig. 11 it is compared the performance of the WGS-based system operating with and without sweep-gas, in terms of global H_2 yield and energy efficiency, both in a normalized way. Operating

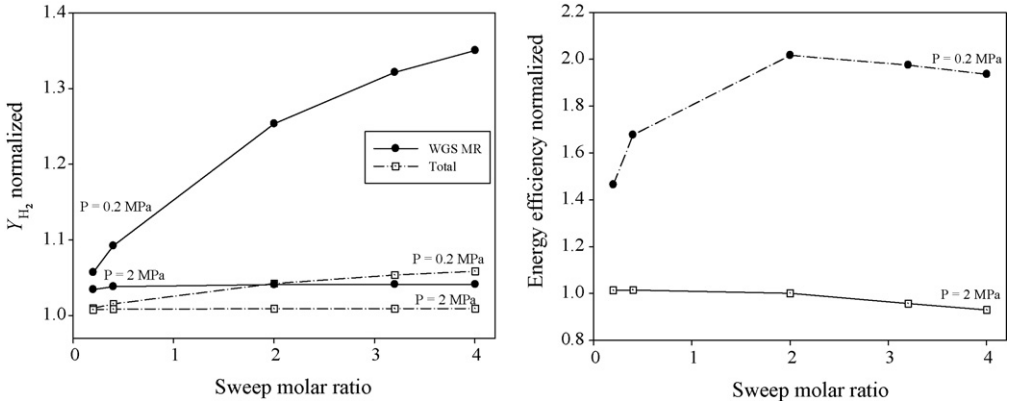

Fig. 11. Comparison of WGS-MR system performance operating with and without steam sweep-gas in terms of the reactor's yield and global energy efficiency. Variables are normalized by the performance of the system without sweep-gas. Other conditions are: T_{Ref} = 700 °C, R = 3 and T_{MR} = 360 °C.

at low pressures, some improvements on the global performance are possible to obtain using a WGS-MR operating with sweep-gas. In particular, the energy efficiency can achieve twice as much the one with no sweep-gas. These differences vanish if higher reaction pressures are used. In fact, at $P_{reaction}$ = 2 MPa the H_2 yields in both systems are similar. On the other hand, at $P_{reaction}$ = 2 MPa the usage of sweep-gas at relatively high sweep molar ratios results in a lower energy efficiency (cf. Fig. 11).

4. Conclusions

A PEMFC/fuel processor stationary system fed with ethanol has been simulated using HYSYS process simulator. The conventional configuration of a fuel processor was compared with a configuration using a WGS Pd–Ag membrane reactor, in terms of hydrogen yield and energy efficiency. The influence of several variables was simulated and discussed, showing the importance of analysing the integrated systems.

Comparing both configurations, it was found that similar energy efficiencies can be obtained if the membrane-based system runs under conditions that favor high H_2 recovery. This can be achieved operating at elevated reaction pressure with no sweep-gas or, alternatively, with low lumen (retentate) pressure but with steam sweep in counter-current mode.

In the membrane reactor configuration, a maximum efficiency of 30.2% is attained at the minimum temperature of the reformer considered in this study (500 °C). The membrane reactor should operate at an optimum temperature of 360 °C in order to attain a compromise between maximum CO conversion and H_2 recovery, thus improving the H_2 yield of the processor and the energy efficiency of the system.

The results obtained show that the usage of water vapor as sweep-gas improves the H_2 yield of the processor in a large range of operating conditions. In terms of energy efficiency of the system, this still holds for low pressures ($P_{reaction}$ < 0.5 MPa), but the improvements are marginal and restricted to a narrower range of conditions at high pressures.

Finally, it was shown that the MR-based fuel cell system is more suitable than the CR one for producing hydrogen under the operating conditions used in this study. The MR-based fuel cell system is simpler than the CR one and shows slightly higher energy efficiencies. Besides, with such a configuration the reduction in system complexity (along with synergetic effects) can be achieved, moving into the logic of the process intensification strategy.

Acknowledgments

Diogo Mendes is grateful to the Portuguese Foundation for Science and Technology (FCT) for his doctoral grant (reference: SFRH/BD/22463/2005). The authors from LEPAE also acknowledge the financing from FCT through the projects PTDC/EQU/ERQ/66045/2006 and POCTI/EQU/59345/2004.

References

[1] V.A. Goltsov, T.N. Veziroglu, Int. J. Hydrogen Energy 26 (2001) 909.
[2] G.A. Deluga, J.R. Salge, L.D. Schmidt, X.E. Verykios, Science 303 (2004) 993.
[3] J.D. Holladay, J. Hu, D.L. King, Y. Wang, Catal. Today 130 (2009) 244.
[4] M. Ni, D.Y.C. Leung, M.K.H. Leung, Int. J. Hydrogen Energy 32 (2007) 3238.
[5] D.K. Liguras, D.I. Kondarides, X.E. Verykios, Appl. Catal. B 43 (2003) 345.
[6] A.J. Shaw, K.K. Podkaminer, S.G. Desai, J.S. Bardsley, S.R. Rogers, P.G. Thorne, D.A. Hogsett, L.R. Lynd, Proc. Natl. Acad. Sci. U.S.A. 105 (2008) 13769.
[7] J.P.W. Scharlemann, W.F. Laurance, Science 319 (2008) 43.
[8] P.D. Vaidya, A.E. Rodrigues, Chem. Eng. J. 117 (2006) 39.
[9] J. Shu, B.P.A. Grandjean, A. Vanneste, S. Kaliaguine, Can. J. Chem. Eng. 69 (1991) 1036.
[10] J.N. Armor, J. Membr. Sci. 147 (1998) 217.
[11] E. Kikuchi, Catal. Today 56 (2000) 97.
[12] A.G. Dixon, Int. J. Chem. Reactor Eng. 1 (2003) 1.
[13] A. Basile, F. Gallucci, S. Tosti, Inorganic membranes: synthesis, characterization, applications, in: R. Malada, M. Menendez (Eds.), Membrane Science, Technology, Elsevier, 2008, p. 255.
[14] J. Sousa, L. Madeira, J. Santos, A. Mendes, in: A. Basile, F. Galluci (Eds.), Modelling and Simulation of Membrane Reactors, Nova Science Publishers, New York, 2009, p. 193.
[15] K. Kordesch, G. Simader, Fuel Cells and Their Applications, Wiley-VCH, Weinheim, 1996.
[16] S. Tosti, L. Bettinali, J. Mater. Sci. 39 (2004) 3041.
[17] S. Tosti, L. Bettinali, D. Lecci, F. Marini, V. Violante, Method of bonding thin foils made of metal alloys selectively permeable to hydrogen, particularly providing membrane devices, and apparatus for carrying out the same, Eur Patent EP 1184125 (2001).
[18] S. Tosti, A. Basile, L. Bettinali, F. Borgognoni, F. Chiaravalloti, F. Gallucci, J. Membr. Sci. 284 (2006) 393.
[19] S. Tosti, L. Bettinali, S. Castelli, F. Sarto, S. Scaglione, V. Violante, J. Membr. Sci. 196 (2002) 241.
[20] S. Tosti, A. Basile, L. Bettinali, F. Borgognoni, F. Gallucci, C. Rizzello, Int. J. Hydrogen Energy 33 (2008) 5098.
[21] P. Bernardo, G. Barbieri, E. Drioli, Chem. Eng. Res. Des. 84 (2006) 405.
[22] J. Godat, F. Marechal, J. Power Sources 118 (2003) 411.
[23] HYSYS Process Simulator Version 3.2, Hyprotech Ltd., Calgary, Canada, 2003.
[24] T. Ioannides, J. Power Sources 92 (2001) 17.
[25] V. Mas, R. Kipreos, N. Amadeo, M. Laborde, Int. J. Hydrogen Energy 31 (2006) 21.
[26] S.Q. Song, S. Douvartzides, P. Tsiakaras, J. Power Sources 145 (2005) 502.
[27] T.A. Semelsberger, L.F. Brown, R.L. Borup, M.A. Inbody, Int. J. Hydrogen Energy 29 (2004) 1047.
[28] J.M. Moe, Chem. Eng. Prog. 58 (1962) 33.
[29] J.M. Thomas, W.J. Thomas, Principles and Practice of Heterogeneous Catalysis, Wiley-VCH, Weinheim, Germany, 1997.
[30] D. Mendes, A. Mendes, L.M. Madeira, A. Iulianelli, J.M. Sousa, A. Basile, Asia-Pac. J. Chem. Eng.\ 5 (2009) 111.
[31] S. Tosti, F. Borgognoni, C. Rizzello, V. Violante, Asia-Pac. J. Chem. Eng. 4 (2009) 369.
[32] W.F. Podolski, Y.G. Kim, Ind. Eng. Chem. Proc. Des. Dev. 13 (1974) 415.
[33] R. Farrauto, S. Hwang, L. Shore, W. Ruettinger, J. Lampert, T. Giroux, Y. Liu, O. Ilinich, Annu. Rev. Mater. Res. 33 (2003) 1.
[34] J.A. Francesconi, M.C. Mussati, R.O. Mato, P.A. Aguirre, J. Power Sources 167 (2007) 151.
[35] A.F. Ghenciu, Curr. Opin. Solid State Mater. Sci. 6 (2002) 389.
[36] D.L. Trimm, Z.I. Onsan, Catal. Rev. -Sci. Eng. 43 (2001) 31.
[37] P. Giunta, C. Mosquera, N. Amadeo, M. Laborde, J. Power Sources 164 (2007) 336.
[38] M. Benito, R. Padilla, J.L. Sanz, L. Daza, J. Power Sources 169 (2007) 123.
[39] A. Perna, Int. J. Hydrogen Energy 32 (2007) 1811.
[40] R. Dittmeyer, V. Hollein, K. Daub, J. Mol. Catal. A: Chem. 173 (2001) 135.
[41] S. Battersby, P.W. Teixeira, J. Beltramini, M.C. Duke, V. Rudolph, J.C.D. da Costa, Catal Today 116 (2006) 12.
[42] R. Hughes, Membr. Technol. 2001 (2001) 9.